

Conserved-mass aggregation model with mass-dependent diffusion rate on complex networks

Sungchul Kwon, Dong-Jin Lee, and Yup Kim*

Department of Physics and Research Institute for Basic Sciences, Kyung Hee University, Seoul 130-701, Korea

(Received 27 January 2009; published 18 June 2009)

We investigate the condensation phenomena of conserved-mass aggregation (CA) with mass-dependent diffusion rate on scale-free networks (SFNs). In the model, the mass m of a node isotropically diffuses to one of directly linked nodes with rate $D(m)=m^{-\alpha}$, where $\alpha>0$. With rate ω , unit mass is chipped from the mass and also isotropically diffuses. It was shown that no condensation phase transitions occur on regular lattices. However, on SFNs with degree distribution $P(k)\sim k^{-\gamma}$, we show from mean-field approximation that the model exhibits various types of condensation phenomena according to α and γ . There exists crossover $\alpha_c=(\gamma-2)/(\gamma-1)$ over which a system undergoes the same type of the condensation as that of zero-range process with jumping rate $p(m)=m^\delta$ regardless of $\gamma(>2)$. We find $\delta=1-\alpha$ for $\alpha_c\leq\alpha<1$ and $\delta=0$ for $\alpha\geq 1$. For $\alpha<\alpha_c$, however, the diffusion of masses cannot be ignored and so a system exhibits different behavior according to the network structure, i.e., γ . For $\gamma>3$, a system exhibits the behavior on regular lattice. For $\gamma\leq 3$, the condensation always occurs for any density with non-power-law background mass distribution. We also numerically confirm the mean-field predictions. Therefore, the network structure leads to the various condensation phenomena of the CA model unlike on regular lattices.

DOI: 10.1103/PhysRevE.79.061115

PACS number(s): 02.50.-r, 89.75.Hc, 05.40.-a, 64.60.Ht

I. INTRODUCTION

Nonequilibrium condensation phenomena have been observed in a wide variety of transport systems ranging from traffic flow to polymer gels [1–8]. These systems evolve via basic microscopic dynamics ubiquitous in nature such as diffusion, aggregation upon contact, and fragmentation of aggregates.

The nonequilibrium steady states of these systems can be classified into two types of phases: the condensed phase and the fluid phase, respectively. In the condensed phase, a finite fraction of total particles condenses on a single site (infinite aggregate). On the other hand, particles are uniformly distributed without an infinite aggregate in the fluid phase. As the rates of dynamic processes vary, a system may undergo the condensation transitions between the two phases at a certain critical density of particles ρ_c [9–13].

The simplest mass-transport model exhibiting the condensation is zero-range process (ZRP) [9]. In ZRP, each site i may contain an integer number of particles m_i and each particle jumps to one of the nearest neighboring sites with jumping rate $p_i(m_i)$. The mass-dependent jumping rate reflects the interaction between particles occupying the same site and describes various condensations such as traffic jam [1], bunching of buses [2], and coalescence of shaken steel balls [3]. On scale-free networks, recent studies showed that the ZRP with jumping rate $p(m)=m^\delta$ exhibits the nontrivial dependence of the condensation on the network properties [10,11].

Another important class of condensation phenomena has been observed in various physical situations such as polymer gels [4], the formation of colloidal suspensions [5], river networks [6,7] and cloud formation [8]. These systems include the microscopic processes of diffusion, aggregation upon

contact, and fragmentation of masses. Conserved-mass aggregation (CA) model is the simplest model incorporating these microscopic processes [12–18]. In one-dimensional CA model, each site may have an integer mass. The mass m_i of a site i moves either to site $i-1$ or to site $i+1$ with unit rate; then $m_i\rightarrow 0$ and $m_{i\pm 1}\rightarrow m_{i\pm 1}+m_i$ (diffusion). With rate ω , unit mass chips off from site i and moves to one of the nearest neighboring sites; $m_i\rightarrow m_i-1$ and $m_{i\pm 1}\rightarrow m_{i\pm 1}+1$ (chipping). The chipping is the special case of the fragmentation which allows the breakup of more than unit mass. The generalization to higher dimensions including the fragmentation is straightforward.

As total masses are conserved, the total density ρ and the rate ω determine the phase of the CA model. The condensation transition arises from the competition between diffusion and chipping process. It was shown that the existence of the condensation transitions depends on the spatial disorder [14], the symmetry of moving directions [15], the constraints on the rate of diffusion and fragmentation [16,17], and also the underlying network structure [18–20].

The prototype of the CA model is the symmetric CA (SCA) model in which the directions of diffusion and chipping processes are isotropic [12,13]. In the SCA model, the single-site mass distribution $P(m)$ was shown to undergo phase transitions on regular lattices [12]. For a fixed ω , as ρ varies across the critical value $\rho_c(\omega)$, the behavior of $P(m)$ for large m was found to be [12]

$$P(m) \sim \begin{cases} e^{-m/m^*} & \rho < \rho_c(\omega) \\ m^{-\tau} & \rho = \rho_c(\omega) \\ m^{-\tau} + \text{infinite aggregate} & \rho > \rho_c(\omega), \end{cases} \quad (1)$$

where $\rho_c(\omega)=\sqrt{\omega+1}-1$ and $\tau=5/2$. ρ_c and τ are independent of the spatial dimension d [13].

In realistic situations such as polymers in solution undergoing the gelation transitions, the diffusion of polymers may depend on their masses which leads to studies on the mass-

*Corresponding author; ykim@khu.ac.kr

dependent diffusion of polymers [16,21,22]. For the SCA model on regular lattices, it was shown that when the diffusion rate depends on mass as $D(m) \sim m^{-\alpha}$, with $\alpha > 0$, the model exhibits different behavior according to α . For $0 < \alpha < 2$, a finite-sized system undergoes the condensation transition of Eq. (1). However, the ρ_c diverges with the volume of system V as $\rho_c \sim V^\beta$ with $\beta = \alpha/(2-\alpha)$. As a result, the condensed phase eventually disappears in the thermodynamic limit $V \rightarrow \infty$ so a system is always in the fluid phase [16]. On the other hand, for $\alpha \geq 2$, the diffusion of masses is negligible and so the model exhibits the behavior of $\alpha = \infty$. The $\alpha = \infty$ case is a ZRP in which unit mass is chipped from mass $m (> 2)$ with rate ω . It was shown for $\alpha = \infty$ that masses are uniformly distributed with $P(m, \rho) \approx e^{-m/\rho}/m$ without the transitions [16].

Critical phenomena on complex networks have been extensively studied because the interplay between particle interaction and underlying network structure leads to the anomalous behavior distinct from standard mean-field behaviors on regular lattices [23]. On scale-free networks (SFNs), it was shown that ZRP [10,11] and CA models [18–20] also exhibit the anomalous condensation transitions distinct from those on regular lattices. These mass-transporting models may model the transmission of data packets between computers. For instance, in ZRP, the fragmentation rate $p(n)$ corresponds to the amount of data packets that can be handled in unit time [10]. In CA model, the diffusion rate may model the time needed to process all data packets of each node.

In this paper, we study the CA model with mass-dependent diffusion rate on SFNs and investigate the effect of the network structure on the condensation phenomena as the natural extension of previous studies [16,18–20]. As the diffusion rate depends on the mass of polymers in polymer gelation transitions, the speed of processing all data packets also depends on the total amount of packets. We consider the diffusion rate of $D(m) = m^{-\alpha}$, with $\alpha > 0$ as in [16]. As we shall see, the interplay between the mass-dependent diffusion rate and the structure of SFNs leads to two types of condensations and the nontrivial crossover between them according to α and γ .

From a mean-field-type balance equation for the mass of an aggregate, we examine the stability of an aggregate against diffusion, i.e., α . We show that on SFNs with the degree exponent γ , there exists a crossover $\alpha_c = (\gamma - 2)/(\gamma - 1)$ over which the diffusive motion of masses is negligible. Intriguingly, α_c varies with γ unlike on regular lattices. Furthermore, as γ decreases, α_c also decreases. Hence, as the inhomogeneity of network structure increases, the diffusion of masses is more suppressed.

For $\alpha < \alpha_c$, the diffusive motions of masses cannot be ignored and the SCA model exhibits different behavior according to γ . For $\gamma > 3$, the model exhibits the same type of behavior as that on regular lattices. However, for $\gamma \leq 3$, the condensation always occurs for any density as the ordinary SCA model of $\alpha = 0$ due to the strong inhomogeneity of degree distribution [18]. It means that the weak diffusion of $\alpha > 0$ does not affect the behavior of $\alpha = 0$ on SFNs with $\gamma \leq 3$.

On the other hand, for $\alpha \geq \alpha_c$, the diffusion of masses is negligible and the SCA model is effectively mapped onto the

ZRP with jumping rate $p(m) = m^\delta$, with $\delta \geq 0$ [10]. Unlike on regular lattices, the steady state of $\alpha \geq \alpha_c$ is not described by the ZRP with constant jumping rate on SFNs. To see the mapping to the ZRP for $\alpha \geq \alpha_c$, we consider the mass δm_D diffusing out from a node with mass m in unit time. With diffusion rate $D(m) = m^{-\alpha}$, δm_D is given by $\delta m_D = m^{1-\alpha}$. Since δm_D always satisfies $\delta m_D \leq m$, the diffusion can be thought as fragmentation of mass δm_D from mass m for $\alpha \geq \alpha_c$. On the other hand, in the ZRP with jumping rate $p(m) = m^\delta$, the mass (particles) δm_C jumping out in unit time is given by $\delta m_C = m^\delta$ [10,11]. Hence the mass δm_D corresponds to δm_C in ZRP with jumping rate $p(m) = m^{1-\alpha}$ in addition to the chipping process of unit mass ($\delta m_C = 1$) with rate ω . As a result, for $\alpha \geq \alpha_c$, two jumping processes compete with each other so the resultant steady state is characterized by the dominant one. For $\alpha \geq 1$, we have $\delta m_D \leq 1$ so the chipping process is dominant; $\delta = 0$ for $\alpha \geq 1$. As a result, the SCA model exhibits the same type of condensation as that of the ZRP with constant jumping rate. However, for $\alpha_c \leq \alpha < 1$, because of $\delta m_D > 1$, the jumping process with rate $p(m) = m^{1-\alpha}$ is dominant; $\delta = 1 - \alpha$ for $\alpha_c \leq \alpha \leq 1$. Therefore, the SCA model exhibits the same type of the condensation as that of the ZRP with the jumping rate $p(m) = m^{1-\alpha}$.

The paper is organized as follows. We introduce the SCA model on SFNs in Sec. II. We discuss the condensation phenomena of the SCA model on SFNs in Sec. III and present simulation results in Sec. IV. Finally, we summarize our results in Sec. V.

II. SCA MODEL WITH DIFFUSION RATE $D(m) = m^{-\alpha}$ ON SCALE-FREE NETWORKS

We consider a network with N nodes and K links. The degree k_i of a node i is defined as the number of links connected to other nodes. The average degree of a node $\langle k \rangle$ is given as $\langle k \rangle = 2K/N$. The degree distribution $P(k)$ is a power-law distribution of $P(k) \sim k^{-\gamma}$ for SFNs. For the construction of SFN, we use a static model [24] instead of preferential attachment algorithm [25]. N nodes are indexed by an integer $i (i = 1 \dots N)$. The weight $p_i = i^{-\lambda}$ is assigned to each node, where λ is a control parameter in $[0, 1)$. Next select two different nodes i and j with probabilities $p_i / \sum_1^N p_k$ and $p_j / \sum_1^N p_k$ and add a link between them unless a link already exists. We repeat this process until the number of total links is K . The degree exponent γ is given as $\gamma = (1 + \lambda) / \lambda$ [24]. In static model, it is desired to use large $\langle k \rangle$ to construct fully connected networks. In simulations, we use $\langle k \rangle = 4$.

The SCA model with diffusion rate $D(m) = m^{-\alpha}$ is defined on SFNs as follows. Each node may have an integer number of particles and the mass on a node is defined as the number of particles on the node. Initially M particles are randomly distributed over N nodes with a given conserved density $\rho = M/N$. Next a node i with mass m_i is randomly chosen. A node j among the nodes directly linked to node i is also chosen randomly. Then one of the following events occurs:

- (i) Diffusion. With rate $D(m_i) = m_i^{-\alpha}$, the mass m_i moves to the node j . If the node j already has mass m_j , then the aggregation takes place; $m_i \rightarrow 0$ and $m_j \rightarrow m_j + m_i$.
- (ii) Chipping. With rate ω , unit mass is chipped from m_i and moves to the node j ; $m_i \rightarrow m_i - 1$ and $m_j \rightarrow m_j + 1$.

The $\alpha=0$ case is the ordinary SCA model on SFNs [18]. On SFNs with $\gamma>3$, the ordinary SCA model exhibits the same type of condensation transitions as those on regular lattices. Hence $P(m)$ follows the behavior of Eq. (1) with $\tau=5/2$. However, the critical line $\rho_c(\omega)$ depends on γ [18]. For $\gamma\leq 3$, an infinite aggregate with a finite fraction of total mass always forms for any density due to the strong inhomogeneity of degree distribution. The diffusion of masses also always leads to a background mass distribution. Since the condensation always occurs with a background mass distribution, the condensation for $\gamma\leq 3$ is incomplete unlike in ZRP where no background masses exist (complete condensation).

For $\alpha<0$, an infinite aggregate should always occur for any ρ . It comes from the fact that the mass gain of an infinite aggregate by the diffusion is proportional to $N^{|\alpha|}$. However, an infinite aggregate always losses only unit mass by the chipping process. Hence, once an infinite aggregate is formed, it is always stable against the chipping process. As a result, the complete condensation always occurs for $\alpha<0$. Thus we only consider the cases with $\alpha>0$.

III. CONDENSATION PHENOMENA ON SFNS

On regular lattices, the SCA model with $D(m)=m^{-\alpha}$ exhibits different behavior according to the values of α as mentioned in Sec. I [16]. For $0<\alpha<2$, the diffusion leads to the same type of the transitions with $\tau<2$ as those of the $\alpha=0$ case in finite-size systems. However, the strength of the diffusion is not strong enough to maintain the transitions in the thermodynamic limit. On the other hand, the diffusion can be ignored for $\alpha\geq 2$ and the SCA model is reduced to the ZRP with a constant jumping rate where no condensation takes place on regular lattices [9]. As a result, there exists a crossover α_c over which the diffusion is ignored and so the SCA model is reduced to a ZRP. On SFNs, one also expects the existence of α_c for $\alpha>0$. However, as we shall see, since the degree distribution is not uniform, α_c depends on the degree distribution, i.e., γ .

To find α_c on SFNs, we assume an infinite aggregate with mass m_a on a hub node with the maximal degree k_{\max} in a network. An infinite aggregate always forms and stays on the hub node in ZRP [10], while it diffuses around on a network in CA models [18–20]. Therefore, examining the stability condition of the aggregate against diffusion, one can find α_c on SFNs. To simplify calculation, we only consider an infinite aggregate without background masses which gives higher-order corrections. The mass diffusing out from the hub in unit time is $m_a^{1-\alpha}$, which is less than m_a itself for $\alpha>0$. Therefore, the diffusion can be thought as the fragmentation of mass $m_a^{1-\alpha}$ from m_a . We apply the same method used in the SCA model with mass-dependent fragmentation to the present model as follows [20].

The loss of m_a by diffusion in unit time is $m_a^{1-\alpha}$. The mass $m_a^{1-\alpha}$ moves to one of the linked nodes to the hub with the probability $1/k_{\max}$. Hence, each node linked to the hub has a mass $m_a^{1-\alpha}/k_{\max}$ on average. As we neglect background masses in our calculation, the gain from the linked nodes by the diffusion is given as

$$\sum_{\ell=1}^{k_{\max}} (m_a^{1-\alpha}/k_{\max})^{1-\alpha}/k_{\ell}, \quad (2)$$

where k_{ℓ}^{-1} is the hopping probability from node ℓ to the hub node. We approximate the sum $\sum_{\ell} 1/k_{\ell}$ to the average $\langle \sum_{\ell} 1/k_{\ell} \rangle_{\text{hub}}$. $\langle \dots \rangle_{\text{hub}}$ denotes the average over the nodes linked to the hub. Then we have $\langle \sum_{\ell} 1/k_{\ell} \rangle_{\text{hub}} = k_{\max} \int^{k_{\max}} g(k)/k dk$, where $g(k)$ is the degree distribution of the nodes directly linked to the hub. In the limit $N \rightarrow \infty$, the number of terms (k_{\max}) in the sum diverges, so we approximate $g(k)$ to $P(k)$. Then we have $\langle \sum_{\ell} 1/k_{\ell} \rangle_{\text{hub}} \sim k_{\max} \langle 1/k \rangle$, with $\langle 1/k \rangle = \int^{k_{\max}} P(k)/k dk$. Since $\langle 1/k \rangle$ is finite, we have $\langle \sum_{\ell} 1/k_{\ell} \rangle_{\text{hub}} \sim k_{\max}$. Hence, we approximately obtain the gain (2) as $m_a^{(1-\alpha)^2} k_{\max}^{\alpha}$.

For $m_a^{(1-\alpha)^2} k_{\max}^{\alpha} \geq m_a^{1-\alpha}$, the aggregate on the hub is stable against diffusion. Otherwise the aggregate diffuses around on a network. With $m_a \sim N$ and $k_{\max} \sim N^{1/(\gamma-1)}$ [25], one gets the stability condition of the aggregate on the hub as

$$N^{1-\alpha} \leq N^{(1-\alpha)^2 + \alpha/(\gamma-1)}. \quad (3)$$

From the condition (3), the crossover α_c is given as

$$\alpha_c = (\gamma - 2)/(\gamma - 1). \quad (4)$$

For $\alpha < \alpha_c$, the aggregate on the hub node is unstable against diffusion and one cannot neglect the diffusive motion of masses. On the other hand, for $\alpha \geq \alpha_c$, the aggregate on the hub is stable against diffusion, so one can neglect the diffusive motion of masses. Hence, the SCA model is reduced to a ZRP for $\alpha \geq \alpha_c$. As on regular lattices, the SCA model exhibits the crossover to a ZRP at α_c which varies with γ . In the next two sections we discuss the condensation phenomena of the SCA model and the corresponding ZRP in detail.

A. SCA model for $\alpha < \alpha_c$

We recently showed that the ordinary SCA model on SFNs exhibits different behavior depending on the network structure, i.e., γ [18]. For $\gamma>3$, the fluctuation of degree distribution is not strong enough to change the mean-field behavior on regular lattices. However, for $\gamma\leq 3$, the fluctuation $\langle k^2 \rangle$ diverges and the network structure is highly inhomogeneous in degree distribution (hub structure). As a result, the condensation phenomena on SFNs with $\gamma\leq 3$ are quite different from that on SFNs with $\gamma>3$ [18,20].

Similarly, it is expected that the SCA model with $D(m)=m^{-\alpha}$ exhibits different behavior depending on γ . For $\gamma>3$, the SCA model is expected to exhibit the same type of condensation phenomena as that of regular lattices. Hence, finite-sized systems undergo the condensation transitions at a certain ρ_c , which diverges with network size N as $\rho_c \sim N^{\beta}$, with $\beta = \alpha/(2-\alpha)$ for $0 < \alpha < \alpha_c$. Since ρ_c diverges with N , the transitions eventually disappear in the thermodynamic limit $N \rightarrow \infty$.

On the other hand, for $\gamma\leq 3$, the ordinary SCA model with $\alpha=0$ exhibits the incomplete condensation with a finite background mass distribution for any mass density ρ [18]. Due to the hub structure, the chipping process, in addition to diffusion, also leads to the condensation unlike on SFNs with

$\gamma > 3$ where the chipping processes scatter masses to lead the fluid phase. Therefore, there are no processes to prevent the condensation on SFNs with $\gamma \leq 3$. However diffusing aggregates scatter masses over a network via chipping processes. As a result, a stable background mass distribution emerges. Since the background distribution should exist for any diffusion rate, one also expects the incomplete condensation on SFNs with $\gamma \leq 3$ for $0 < \alpha < \alpha_c$.

B. Mapping onto a ZRP for $\alpha \geq \alpha_c$

For $\alpha \geq \alpha_c$, one can neglect the diffusion of masses, so the SCA model is mapped onto a ZRP with a certain jumping rate. For the mapping to a ZRP, we consider the mass δm_D diffusing out from a node with mass m in unit time. With diffusion rate $D(m) = m^{-\alpha}$, δm_D is given by $\delta m_D = m^{1-\alpha}$, which is less than the total mass m itself for $\alpha > 0$. Therefore, the diffusion can be thought as the fragmentation of mass $m^{1-\alpha}$ from a node with mass m . On the other hand, in the ZRP with jumping rate $p(m) = m^\delta$, the mass (particle) δm_C jumping out in unit time is given by $\delta m_C = m^\delta$ [10,11]. Since the diffusion corresponds to the fragmentation for $\alpha \geq \alpha_c$, the mass δm_D can be thought as δm_C in the ZRP with jumping rate $p(m) = m^{1-\alpha}$.

In addition to the diffusion, there is the chipping process of unit mass ($\delta m_C = 1$) with rate ω which corresponds to the jumping rate $P(m) = \omega$, i.e., $\delta = 0$. As a result, for $\alpha \geq \alpha_c$, the SCA model is mapped onto the ZRP with two jumping rates $p(m) = m^{1-\alpha}$ and $p(m) = \omega$. The two jumping processes compete with each other, so the resultant steady state of $\alpha \geq \alpha_c$ is characterized by the dominant one.

For $\alpha \geq 1$, we have $\delta m_D \leq 1$ so the chipping process (unit-mass dissociation) is dominant; $\delta = 0$ for $\alpha \geq 1$. As a result, the SCA model exhibits the same type of condensation as that of the ZRP with constant jumping rate for $\alpha \geq 1$. However, for $\alpha_c \leq \alpha < 1$, because of $\delta m_D > 1$, the jumping process with rate $p(m) = m^{1-\alpha}$ is dominant; $\delta = 1 - \alpha$ for $\alpha_c \leq \alpha < 1$. Therefore, the SCA model exhibits the same type of the condensation as that of the ZRP with $p(m) = m^{1-\alpha}$ for $\alpha_c \leq \alpha < 1$.

On SFNs with $\gamma > 2$, the ZRP with $p(m) = m^\delta$ undergoes the complete condensation for any ρ when $0 \leq \delta < \delta_c = 1/(\gamma - 1)$ [10]. For $\delta \geq \delta_c$, the condensation does not occur. In the present model, the crossover δ_c is given as $\delta_c = 1 - \alpha_c = 1/(\gamma - 1)$ over which the mapping to the ZRP is lost. The same δ_c of the present model and the ZRP of [10] reflects that our mapping to the ZRP is correct for $\alpha \geq \alpha_c$. In the ZRP with $p(m) = m^\delta$, the average mass m_k of a node with degree k exhibits different behavior according to δ [10]. For $\delta < \delta_c$, m_k scales with degree k as $m_k = (k/k_c)$ for $k \leq k_c$ and $m_k = (k/k_c)^{1/\delta}$ for $k \geq k_c$. k_c is a certain crossover degree at which $m_k = 1$ [10]. Especially at $\delta = 0$, m_k linearly increases until $k < k_{\max}$ and jumps to the value $m^* \approx \rho N$ at k_{\max} .

In the SCA model of $\alpha \geq \alpha_c$, one also expects the crossover of m_k at a certain k'_c . For $\alpha \geq 1$, $p(m)$ is a constant, so m_k scales as $m_k \sim k$ and jumps to $m^* \approx \rho N$ at k_{\max} . For $\alpha_c \leq \alpha < 1$, the jumping rate $p(m) = m^{1-\alpha}$ should lead to the crossover of m_k at a certain k'_c , i.e., $m_k \sim k$ for $k \leq k'_c$ and $m_k \sim k^{1/(1-\alpha)}$ for $k \geq k'_c$. However, m_k for small masses is ex-

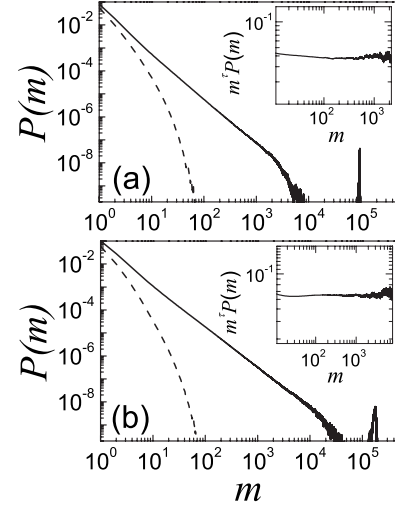


FIG. 1. The plot of $P(m)$ for $\alpha < \alpha_c = 2/3$ on SFNs with $\gamma = 4$. The main plots show $P(m)$ for (a) $\alpha = 0.1$ and (b) 0.3 with $\omega = 1$ and $N = 10^4$. Solid and dashed lines correspond to (a) $\rho = 10$ and 0.1 and (b) $\rho = 20$ and 0.1 , respectively. In each panel, inset shows the scaling plot $m^\tau P(m)$, with (a) $\tau = 1.91$ and (b) 1.76 .

pected to follow the behavior of the SCA model because one cannot neglect the diffusion of small masses. Hence, the mapping to the ZRP is lost for small masses. In ordinary SCA model [18], m_k scales as $m_k = \rho k / \langle k \rangle$ [26]. Hence, we expect $m_k = \rho k / \langle k \rangle$ for $k \leq k'_c$. From $m_k = \rho k / \langle k \rangle$ for $k \leq k'_c$ and $m_k = (k/k_c)^{1/(1-\alpha)}$ for $k \geq k'_c$, one finds k'_c as $k'_c \sim (k_c)^{1/\alpha}$. Because of $\alpha < 1$, k'_c is larger than that of the ZRP.

IV. MONTE CARLO SIMULATION RESULTS

A. For $\alpha < \alpha_c$

We simulate the SCA model with $D(m) = m^{-\alpha}$ on SFNs of size N up to 2×10^4 . We set the average degree $\langle k \rangle = 4$. We also set $\omega = 1$ for all simulations. We run simulation up to 10^7 Monte Carlo time steps and measure $P(m)$ in the steady state. For $\alpha < \alpha_c$, the SCA model is expected to exhibit the mean-field behavior on regular lattices for $\gamma > 3$, while the incomplete condensation always takes place for $\gamma \leq 3$.

First, we consider the SCA model on SFNs with $\gamma > 3$. Hence, finite-sized systems undergo the condensation phase transition from the fluid phase into the condensed phase at a certain critical density ρ_c which diverges with network size N as $\rho_c \sim N^\beta$, with $\beta = \alpha / (2 - \alpha)$ [16]. We perform simulations on SFNs with $\gamma = 4$ with $\alpha = 0.1$ and 0.3 . Figure 1 shows $P(m)$ for $N = 10^4$. As shown, $P(m)$ undergoes the condensation transition of Eq. (1) at a certain ρ_c for both α values. Using the scaling plot of $m^\tau P(m)$, we estimate $\tau = 1.91(5)$ for $\alpha = 0.1$ and $\tau = 1.76(5)$ for $\alpha = 0.3$, respectively (insets of Fig. 1). Compared to the mean-field τ , $\tau = 2 - \alpha/2$ [16], our estimates agree well with the mean-field value $\tau = 1.9$ for $\alpha = 0.1$ and 1.7 for $\alpha = 0.3$, respectively. As on regular lattices, τ is smaller than 2, which indicates a diverging ρ_c with N [16]. Therefore, the condensation transition eventually disappears in the thermodynamic limit $N \rightarrow \infty$.

To estimate ρ_c , we use the following method [17,20]. In the steady state, $P(m)$ scales as [13]

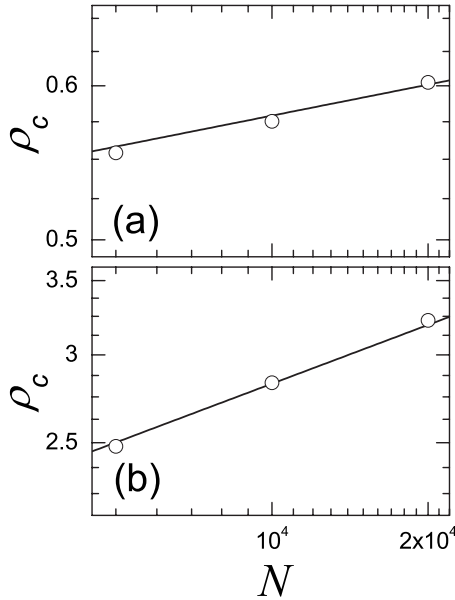


FIG. 2. The plot of $\rho_c(N)$ for $\alpha < \alpha_c = 2/3$ on SFNs with $\gamma = 4$. In each panel, the symbols correspond to ρ_c of (a) $\alpha = 0.1$ and (b) 0.3 for various N from 5×10^3 to 2×10^4 . In each panel, solid line corresponds to the line with the slope $\beta = \alpha / (2 - \alpha)$.

$$P(m) = m^{-\tau} f(m/N^\phi) + \frac{1}{N} \delta [m - (\rho - \rho_c)N]. \quad (5)$$

From the conservation of total masses, ρ_c is given as $\rho_c = \rho - \rho_\infty$, where ρ_∞ is the density of an infinite aggregate. The exponent ϕ is the crossover exponent [13]. From the fact that the background distribution does not change for $\rho \geq \rho_c$, one can estimate ρ_c from the relation $\rho_c = \int_1^{m_0} m P(m) dm$ in the condensed phase, where m_0 is the cutoff mass at which the background distribution terminates.

We measure $P(m)$ in the condensed phase with $\rho = 10$ and N up to 2×10^4 for $\alpha = 0.1$ and 0.3 . With the method discussed above, we measure ρ_c and plot in Fig. 2. All the data in Fig. 2 satisfy the mean-field result $\rho_c \sim N^\beta$, with $\beta = \alpha / (2 - \alpha)$ very well [16]. Therefore, we conclude that the SCA model with $\alpha < \alpha_c$ follows the mean-field behavior of [16] on SFNs with $\gamma > 3$ as expected.

For $\gamma \leq 3$, the incomplete condensation is expected to occur for any ρ . For $\gamma = 2.8$, we measure $P(m)$ with $\alpha = 0.1$. In Fig. 3, we plot $p(m)$ with $\rho = 1.0$ for various N up to 2×10^4 . As shown, the condensation occurs, but $P(m)$ is neither simple power law nor simple exponential. We call the $P(m)$ quasiexponential [20]. The cutoff mass m_0 increases with N , which indicates the background distribution is stable in the thermodynamic limit. The background mass density ρ_b defined as $\rho_b = \sum^{m_0} m P(m)$ tends to saturate to a finite value (inset of Fig. 3). The finite ρ_b and the quasiexponential $P(m)$ characterize the incomplete condensation [20]. Therefore, we are convinced that the incomplete condensation always occurs for $\gamma \leq 3$ and $\alpha < \alpha_c$.

B. For $\alpha \geq \alpha_c$

For $\alpha \geq \alpha_c$, the present model is mapped onto the ZRP with jumping rate $p(m) = m^\delta$. The exponent δ is given as

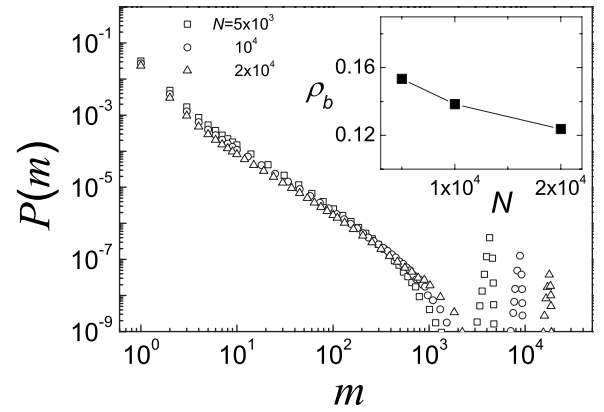


FIG. 3. The plot of $P(m)$ for $\alpha = 0.1$ on SFNs with $\gamma = 2.8$. Inset shows ρ_b for various N .

$\delta = 1 - \alpha$ for $\alpha_c \leq \alpha < 1$ and $\delta = 0$ for $\alpha \geq 1$. Since the complete condensation always occurs in the ZRP on SFNs with $\gamma > 2$ [10], the $P(k)$ distribution only changes the $\alpha_c = (\gamma - 2) / (\gamma - 1)$. For $\alpha_c \leq \alpha < 1$, the average mass m_k of a node with degree k linearly increases with k for $k \leq k'_c$ and algebraically increases as $k^{1/(1-\alpha)}$ for $k \gg k'_c$. k'_c is the crossover degree of the present model. For $\alpha \geq 1$, m_k linearly increases until $k < k_{\max}$ and jumps to the value $m^* \approx \rho N$ at k_{\max} . We simulate the SCA model on SFNs with $\gamma = 4$ and 2.8 , where $\alpha_c = 2/3$ for $\gamma = 4$ and $\alpha_c \approx 0.44$ for $\gamma = 2.8$, respectively.

For $\alpha_c \leq \alpha < 1$, we run simulations up to 5×10^4 time steps and measure m_k in the steady state. For $\gamma = 4$, we measure m_k at $\alpha = 0.67 (\approx \alpha_c)$ with $\rho = 1$ and 0.8 with $\rho = 4$. Figure

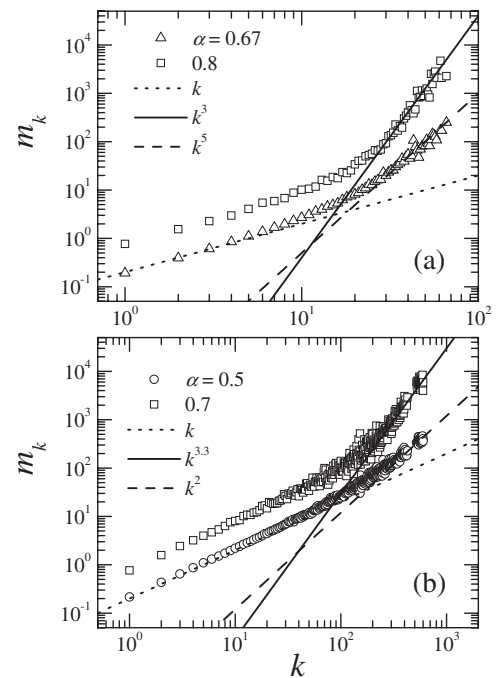


FIG. 4. The plot of m_k . (a) m_k at $\alpha = 0.67$ with $\rho = 1$ and $\alpha = 0.8$ with $\rho = 4$ for $\gamma = 4$. (b) m_k at $\alpha = 0.5$ with $\rho = 1$ and $\alpha = 0.7$ with $\rho = 4$ for $\gamma = 2.8$. In each panel, solid and dashed lines correspond to the line with the slope $1/(1-\alpha)$ with the α of each symbol. Dotted line is the line with unit slope.

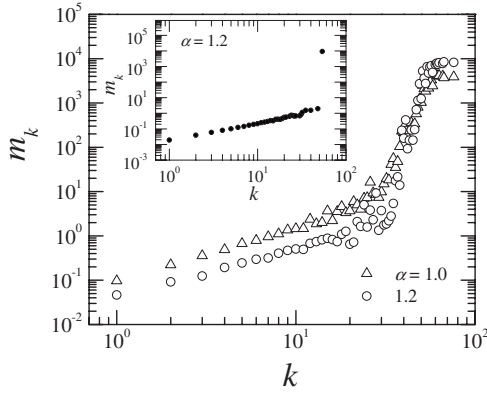


FIG. 5. The plot of m_k for $\alpha=1.0$ and 1.2 with $\rho=1$ on SFNs with $\gamma=4$. Inset shows m_k of a single run with $\alpha=1.2$.

4(a) shows m_k for $\alpha=0.67$ and 0.8 . For $k > k'_c$, the m_k of each α algebraically increases with k as $k^{1/\delta}$ and collapses onto the line with the expected slope $1/\delta=1/(1-\alpha)$, i.e., $1/\delta=5.0$ for $\alpha=0.8$ and $1/\delta\approx 3.0$ for 0.67 , respectively. For $\gamma=2.7$, we measure m_k at $\alpha=0.5$ with $\rho=1$ and 0.7 with $\rho=4$. As expected for $k > k'_c$, m_k of each α collapses onto the line with the expected slope, $1/\delta=2$ for $\alpha=0.5$ and $10/3$ for $\alpha=0.7$ [Fig. 4(b)].

For $\alpha \geq 1$, we measure m_k at $\alpha=1.0$ and 1.2 with $\rho=1$ for $\gamma=4$. We run simulations up to 10^5 time steps and average m_k over 2400 independent runs. As shown in Fig. 5, m_k linearly increases for $k < k_{\max}$ and fast increases to the maximum value $m^* \approx 10^4$ at about $k \approx k_{\max}$. The inset of Fig. 5 shows m_k of a single run at $\alpha=1.2$, which clearly jumps to $m^* \approx 10^4$ at k_{\max} . Sample average smoothes out the jump of m_k at k_{\max} . Since most of masses condense on the hub node, the complete condensation occurs for $\alpha \geq 1$. As a result, the same type of the complete condensation as that of the ZRP with constant jumping rate takes places for $\alpha \geq 1$ as expected.

Finally, we discuss the effect of diffusion of small masses for $\alpha \geq \alpha_c$. For sufficiently small masses with $\delta m_D = m^{1-\alpha} \approx m$ for a given α , one cannot neglect diffusive motions even for $\alpha \geq \alpha_c$ where we neglect the diffusion of big masses. Hence, such a small m_k is expected to follow the behavior of the ordinary SCA model of $\alpha=0$, i.e., $m_k = \rho k / \langle k \rangle$ [18,26]. However, for $\alpha \geq 1$, δm_D always satisfies $\delta m_D \leq 1$, so that the diffusion of all masses is suppressed except $m=1$. Hence, small masses are expected to follow the behavior of $\alpha=0$ for $\alpha < 1$ unlike big masses.

For $\alpha_c \leq \alpha < 1$, we measure m_k for various ρ up to 20 on SFNs with $\gamma=4$ with $\alpha=0.8$ and $N=10^4$. Figure 6(a) shows the dependence of m_k on ρ . In Fig. 6(b), we plot $m_k \langle k \rangle / \rho$ against k , which collapse on a single curve as expected. On the other hand, for $\alpha \geq 1$, as shown in Fig. 5, m_k of $\alpha=1.0$ and 1.2 do not overlap each other despite of the same density, $\rho=1$. It means that the behavior of $\alpha=0$ for small masses disappears for $\alpha \geq 1$ as expected. Therefore, for small masses, the feature of the ordinary SCA model remains for $\alpha < 1$.

V. SUMMARY

In summary, we investigate the condensation phenomena of symmetric SCA with mass-dependent diffusion rate on

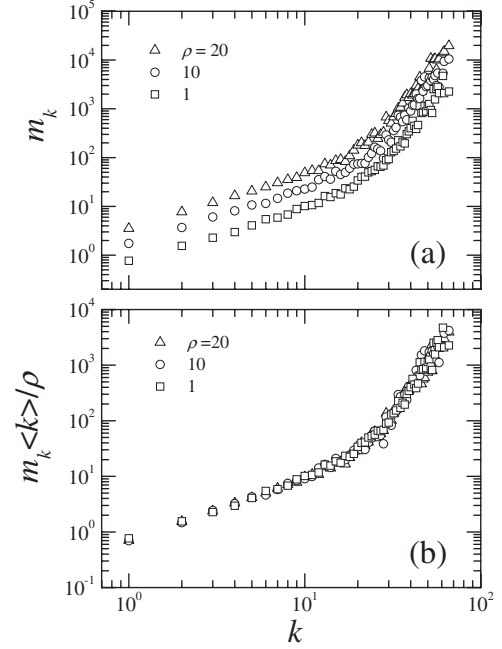


FIG. 6. The plot of m_k for $\alpha=0.8$ and $\gamma=4$. (a) Each symbol corresponds to m_k of $\rho=1, 10$, and 20 , respectively. (b) $m_k \langle k \rangle / \rho$ of each ρ collapses on a single curve.

SFNs. In the model, the mass m of a node isotropically diffuses to one of directly linked nodes with rate $D(m)=m^{-\alpha}$, where $\alpha > 0$. With rate ω , unit mass is chipped from the mass and also isotropically diffuses. On regular lattices, it was shown that the SCA model exhibits the crossover to ZRP with constant jumping rate at $\alpha_c=2$ [16]. Hence, for $\alpha \geq \alpha_c$, the diffusion of masses does not affect the steady-state properties.

On SFNs with degree distribution $P(k) \sim k^{-\gamma}$, we show from mean-field approximation that the model exhibits various types of condensation phenomena depending on α and γ . Examining the stability condition of an aggregate on the hub node against diffusion, we find $\alpha_c = (\gamma-2)/(\gamma-1)$ which varies with γ unlike on regular lattices. As the inhomogeneity of network structure increases, the diffusion of masses is more suppressed. For $\alpha \geq \alpha_c$, the diffusion of masses can be ignored, so the SCA model is mapped onto the ZRP with jumping rate $p(m)=m^\delta$ as follows.

The masses δm_D diffusing out from a node in unit time are given by $\delta m_D = m^{1-\alpha}$ in the CA model, while the mass δm_C jumping out from a node in unit time is given by $\delta m_C = m^\delta$ in the ZRP. Comparing δm_D to δm_C , we find the exponent δ for $\alpha \geq \alpha_c$ as $\delta=1-\alpha$ for $\alpha \leq \alpha < 1$ and $\delta=0$ for $\alpha \geq 1$. As in the ZRP on SFNs [10], the average mass m_k of a node with degree k exhibits the crossover from linear increase to algebraic increase as $k^{1/(1-\alpha)}$ at a certain k_c for $\alpha_c \leq \alpha < 1$. However, for $\alpha \geq 1$, m_k linearly increases until the maximal degree k_{\max} and jumps at k_{\max} . We numerically confirm the behavior of m_k for different γ values.

For $\alpha < \alpha_c$, however, the diffusion of masses cannot be ignored, which leads to the different condensation phenomena according to the network structure, i.e., γ . For $\gamma > 3$, a system exhibits the mean-field behavior on regular lattices.

Hence, finite-sized systems undergo the condensation transition at a certain ρ_c , which diverges with network size N as N^β , with $\beta=\alpha/(2-\alpha)$ as on regular lattices. As a result, the condensation transition eventually disappears in the thermodynamic limit. However, for $\gamma\leq 3$, due to the strong inhomogeneity of degree distribution, the condensation always occurs for any density as in the ordinary SCA model with $\alpha=0$ [18]. We numerically confirm the mean-field predictions for $\gamma>3$ and the existence of the incomplete condensation for $\gamma\leq 3$. The interplay of the diffusion rate and the network structure leads to the rich

behaviors of the SCA model which are not observed on regular lattices.

ACKNOWLEDGMENTS

This work was supported by the Korea Science and Engineering Foundation (KOSEF) grant funded by the Korean Government (MOST) (Grant No. R01-2007-000-10910-0) and by the Korea Research Foundation Grant funded by the Korean Government (MOEHRD, Basic Research Promotion Fund) (Grant No. KRF-2007-313-C00279).

-
- [1] M. R. Evans, *Europhys. Lett.* **36**, 13 (1996).
 [2] O. J. O'Loan, M. R. Evans, and M. E. Cates, *Phys. Rev. E* **58**, 1404 (1998).
 [3] D. van der Meer *et al.*, *J. Stat. Mech.: Theory Exp.* (2004), P04004; J. Torok, e-print arXiv:cond-mat/0407567.
 [4] R. M. Ziff, *J. Stat. Phys.* **23**, 241 (1980).
 [5] W. H. White, *J. Colloid Interface Sci.* **87**, 204 (1982).
 [6] A. E. Scheidegger, *Bull. I.A.S.H.* **12**, 15 (1967).
 [7] A. Maritan, A. Rinaldo, R. Rigon, A. Giacometti, and I. Rodriguez-Iturbe, *Phys. Rev. E* **53**, 1510 (1996); M. Cieplak, A. Giacometti, A. Maritan, A. Rinaldo, I. R. Iturbe, and J. R. Banavar, *J. Stat. Phys.* **91**, 1 (1998).
 [8] S. K. Friedlander, *Smoke, Dust and Haze* (Wiley Interscience, New York, 1977).
 [9] M. R. Evans, *Braz. J. Phys.* **30**, 42 (2000); M. R. Evans and T. Hanney, *J. Phys. A* **38**, R195 (2005).
 [10] J. D. Noh, G. M. Shim, and H. Lee, *Phys. Rev. Lett.* **94**, 198701 (2005); J. D. Noh, *Phys. Rev. E* **72**, 056123 (2005).
 [11] M. Tang, Z. Liu, and J. Zhou, *Phys. Rev. E* **74**, 036101 (2006).
 [12] S. N. Majumdar, S. Krishnamurthy, and M. Barma, *Phys. Rev. Lett.* **81**, 3691 (1998); *J. Stat. Phys.* **99**, 1 (2000).
 [13] R. Rajesh and S. N. Majumdar, *Phys. Rev. E* **63**, 036114 (2001).
 [14] K. Jain and M. Barma, *Phys. Rev. E* **64**, 016107 (2001).
 [15] R. Rajesh and S. Krishnamurthy, *Phys. Rev. E* **66**, 046132 (2002).
 [16] R. Rajesh, D. Das, B. Chakraborty, and M. Barma, *Phys. Rev. E* **66**, 056104 (2002).
 [17] D.-J. Lee, S. Kwon, and Y. Kim, *J. Korean Phys. Soc.* **52**, S154 (2008).
 [18] S. Kwon, S. Lee, and Y. Kim, *Phys. Rev. E* **73**, 056102 (2006).
 [19] S. Kwon, S. Yoon, and Y. Kim, *Phys. Rev. E* **77**, 066105 (2008).
 [20] S. Kwon, D.-J. Lee, and Y. Kim, *Phys. Rev. E* **78**, 036113 (2008).
 [21] D. J. Aldous, *Bernoulli* **5**, 3 (1999); R. D. Vigil, R. M. Ziff, and B. Lu, *Phys. Rev. B* **38**, 942 (1988); G. Oshanin and M. Moreau, *J. Chem. Phys.* **102**, 2977 (1995).
 [22] M. Doi and S. F. Edwards, *The Theory of Polymer Dynamics* (Oxford University Press, New York, 1986).
 [23] S. N. Dorogovtsev, A. V. Goltsev, and J. F. F. Mendes, *Rev. Mod. Phys.* **80**, 1275 (2008).
 [24] K.-I. Goh, B. Kahng, and D. Kim, *Phys. Rev. Lett.* **87**, 278701 (2001).
 [25] S. N. Dorogovtsev and J. F. F. Mendes, *Adv. Phys.* **51**, 1079 (2002); R. Albert and A.-L. Barabási, *Rev. Mod. Phys.* **74**, 47 (2002).
 [26] In Ref. [18], we omit the normalization factor N from P_k^∞ . With the factor N , one finds $m_k = \rho k / \langle k \rangle$.